Published in final edited form as:
Proc Meet Acoust. 2011 July 10; 11: 020005–020031.

Time-reversal Techniques in Ultrasound-assisted Convection-enhanced Drug Delivery to the Brain: Technology Development and In Vivo Evaluation

George K. Lewis Jr.[*], **Sabrina Guarino**, **Gaurav Gandhi**, **Laurent Filinger**, **George K. Lewis Sr.**, **Willam L. Olbricht**, and **Armen Sarvazyan**

Abstract

We describe a drug delivery method that combines Time-Reversal Acoustics (TRA) with Convection-Enhanced Delivery (CED) to improve the delivery of therapeutics to the interstitium of the brain. The Ultrasound-assisted CED approach (UCED) circumvents the blood-brain barrier by infusing compounds through a cannula that is inserted into the brain while simultaneously delivering ultrasound to improve the penetration of pharmaceuticals. CED without ultrasound-assistance has been used to treat a variety of neural disorders, including glioblastoma multiforme, a malignancy that presents a very poor prognosis for patients. We describe a novel system that is used to infuse fluids into the brain parenchyma while simultaneously exposing the tissue to safe levels of 1-MHz, low intensity, ultrasound energy. The system includes a combined infusion needle-hydrophone, a 10-channel ultralow-output impedance amplifier, a broad-band ultrasound resonator, and MatLab®-based TRA control and user-interface. TRA allows easy coupling of ultrasound therapy through the skull without complex phase-correction and array design. The smart targeting UCED system has been tested in vivo and results show it provides 1.5-mm spatial resolution for UCED and improves tracer distribution in the brain over CED alone.

1. INTRODUCTION

1.1 Convection Enhanced Delivery

Convection Enhanced Delivery (CED) is a means for delivery of a chemotherapeutic agent directly to the brain. It was developed in the early 1990's [1] for the treatment of brain gliomas, but it has also been explored as a method to deliver drugs to treat focal epilepsy [2], spinal cord degeneration [3,4], Parkinson's disease [5,6], and neuronopathic Gaucher's disease [7]. CED uses infusion of therapeutics under a driving pressure, directly into the brain to bypass the blood-brain barrier [1]. The convective driving force of CED can deliver compounds deep within brain parenchyma, which is an important potential advantage over systemic and local diffusion-based delivery. For example, glioblastoma multiforme (GBM) is a highly aggressive and infiltrative tumor; malignant cells migrate away from the main tumor and are left behind following surgical resection of the tumor. Post-resection chemotherapy, radiation and other therapeutic approaches are unable to eliminate all of the remaining malignant cells. As a result, the malignancy grows back, usually within 1 to 3 cm of the original tumor. The typical survival time of patients is about one year after the diagnosis of GBM [8], survival can be extended to a few months longer with some of the

[*]Corresponding author's address: Biomedical Engineering, Cornell University, B60 Weill Hall, Ithaca, NY 14850, george@cornellbme.com.

new treatment approaches. Figure 1 is a diagrammatic example on traditional CED and diffusion-based treatment strategies for GBM.

The extent of infusion in CED is often measured by the distribution volume V_d of the infusate. It can be determined by examining brain slices *post mortem* in animal models or by Computed Tomography and/or Magnetic Resonance Imaging *in vivo*. Figure 2 shows qualitatively V_d as a function of the infused volume V_i for three classes of therapeutics: small molecules, proteins, and nanoparticles. In all cases V_d is close to a linear function of Vi. Small molecules such as sucrose can move unhindered through the extracellular space within the fluid. In this case the slope of the line V_d / V_i approaches $1/\varphi$, where φ is the brain tissue porosity (approximately 0.2). Proteins are larger and may interact physically with extracellular matrix (ECM) components, and are subject to elimination during transit through the interstitium. Therefore, V_d / V_i is smaller and varies with molecular weight, structure, charge, and other factors. The motion of nanoparticles, including liposomes and polymeric spheres, is strongly hindered in the interstitium thus V_d/V_i approaches 0.2. Infusing nanoparticles in a hyperosmolar solution, which draws fluid from capillaries and cells to swell the interstitium and increase porosity, can increase V_d/V_i by a factor of about two [9]. However, greater enhancement is required in practice, which means that new ways must be found to increase the mobility of drugs and nanoparticles in brain parenchyma.

The V_d also is affected by heterogeneities in the brain. For example, the hydraulic conductivities of white and gray matter differ by more than an order of magnitude; white matter easily conducts infused fluid compared with gray matter. As a result, when infusate enters a white matter tract, it can travel great distances within the tract, bypassing gray matter that may contain malignant target cells. Furthermore, the hydraulic conductivity of white matter is anisotropic, and fluid flows preferentially in the direction of neuronal fibers in white matter tracts [10]. The fluid-filled ventricles that are part of the cerebral spinal fluid circulation also affect site-specific V_d. Infused material that enters a ventricle or the resection cavity after surgery is unlikely to return to brain parenchyma and is therefore lost for therapeutic purposes. Thus, techniques are required not only to increase the V_d but also to control the direction of transport, and therefore the shape of the V_d and the fate of the infused material.

1.2 Ultrasound-Assisted Brain Drug Delivery

Ultrasound research for medical bioacoustics effects and drug delivery applications has evolved over several decades, with a recent explosion of ultrasound targeted drug delivery within the last ten years. Sonophoresis and the use of ultrasonic vibrations to enhance drug delivery transdermally has been extensively studied [11–15], yet the treatment approach has not been optimized and made broadly accessible. Ultrasound energy over a wide range of acoustic intensities and frequencies causes increases in the permeability of the stratum corneum and adds kinetic energy to topical therapeutics, allowing and/or mediating transport across skin of therapeutic compounds that would otherwise be excluded. A variety of thermal and non-thermal mechanisms are important, including stable and inertial cavitation, micromixing and streaming [16, 17]. The large pressure forces generated during inertial cavitation bubble implosion activity is still considered to be the dominant mechanism of ultrasound to disrupt the adjacent stratum corneum, opening paths to underlying tissue and capillaries while the oscillation of bubbles causes local mixing. At lower power levels as well, ultrasound can generate stable cavitation and acoustic streaming, which result in local convective motion. High Intensity Focused Ultrasound (HIFU) has been shown as an minimally invasive tool to target specific regions of the body to deliver therapeutic ultrasound levels for ablation and drug delivery [18,19]. Ultrasound mediated disruption of the blood brain barrier using HIFU is being examined to help drugs escape the blood stream and enter the brain by inertial and stable cavitation activity [18]. The use of therapeutic

ultrasound from 85 kHz to 1.5 MHz has shown multi-fold transport enhancement of molecules such as Mannitol (182 Da), Carmustine (220 Da), Doxyrubicin (Evans blue dye (960 Da), Inulin (5kDa), Albumin conjugated Evans blue dye (60 kDa) and Dextran (70 kDa) in agarose, muscle and brain tissue *in vitro* [20, 21, 22] and in the rodent and primate brain *in vivo* [23, 24] at safe ultrasound exposure levels.

1.2.1 Ultrasound-Assisted Diffusion in Brain Tissue—We have found that exposing tissue to ultrasound enhances diffusion of model tracers such as Evans blue dye (EBD) and albumin conjugated Evans blue dye (AcEBD) in tissue phantoms and *ex vivo* brain tissue specimens. For example, exposing agarose 0.6 wt% brain phantoms or *ex vivo* equine brain tissue to 533 kHz or 1.58 MHz ultrasound for only a few minutes provides increased tracer uptake on the order of 2 to 8 fold as compared to diffusion alone [20, 21, 25].

The effect of ultrasound enhanced diffusion and its effect on tracer penetration into tissue can be examined by fitting experimental results to models describing diffusion based brain transport kinetics. One model to measure the concentration profile of a chemotherapeutic diffusing through brain tissue was developed to predict concentrations of Carmustine (BCNU) and other chemotherapeutics released from polymeric wafers implanted in the rat [26] and monkey brain [27]. In this model, brain tissue is considered a medium comprising three phases: extracellular space (ECS), intracellular space (ICS) and cell membrane (CM) [26–28]. The local chemotherapeutic concentration depends on its rate of transport through the tissue, its rate of elimination by degradation, metabolism, and permeation into blood capillaries, and its rate of binding and internalization.

Figure 3 shows an experimental dimensionless concentration profile of Evans Blue Dye (EBD) with and without exposure of the equine brain tissue to 1.58 MHz ultrasound at an intensity of 1 W/cm^2 for 2 min. The rough red curve shows the concentration profile of EBD in the sample without ultrasound (pure diffusion). The rough blue curve shows the concentration profile for tissue exposed to continuous ultrasound. Fluctuations in the measured concentration profiles may have resulted from structural variations in tissue, since these fluctuations are not observed for experiments involving agarose gel brain phantoms.

Under the assumption that ultrasound exposure is not a time dependent effect, and the relativistic changes in ultrasound treated samples vs. non-ultrasound treated diffusion based transport kinetics are similar in the steady-state and time-dependent solutions to the model, we can fit the steady-state model to the experimental data presented by adjusting the diffusion coefficient using a least squared approach (smooth red and blue curves). We can estimate that ultrasound exposure increases the *relative* EBD diffusion coefficient by about a factor of 40 in this case (smooth blue curve). If, the 40-fold increase in the relative diffusion constant could be realized clinically by using ultrasound at safe exposure levels to assist diffusion based strategies, the penetration of chemotherapeutic would be significantly enhanced, which could significantly improve outcomes of the therapy for glioblastoma patients.

1.2.2 Ultrasound-Assisted Convection in Brain Tissue—Convection Enhanced Delivery (CED) can deliver therapeutics locally at concentrations that exceed systemic toxicity limits, but the challenge is to deliver those compounds to specific distant targets that may be selected in pre-treatment planning. For small molecules that are infused using CED, the average convective velocity may be relatively large; however the convective velocity of proteins and nanoparticles is much smaller because their transport is hindered by the pore size of the caudate (approx 100 nm) [29].

Ultrasound in plane wave and focused applications has been shown to enhance convective transport of compounds through muscle and brain tissue *ex vivo* [22, 25], and this effect has been exploited *in vivo* [25]. Experiments have been conducted that show ultrasound can be combined with convection to increase the penetration of tracers in the rodent brain using specially design transducers and cannulas. Ultrasound-assisted Convection Enhanced Delivery (UCED) is employed by performing a small craniotomy on the rodent under anesthesia and infusing with a micro pump at 0.25 to 1 μL/min with simultaneous exposure to 1.34 MHz low intensity ultrasound for the duration of the infusion as shown in Figure 4A. Relativity low acoustic intensities (47–150 mW/cm^2) increase the distribution volume V_d of Evans Blue Dye (EBD) by 1.16 to 3.25 times as compared with control depending on exposure parameters including time, infusion rate and acoustic intensity/duration. The underlying mechanisms are still unresolved however: acoustic streaming, mechanical wave interaction with the poroelastic matrix, increased tissue permeability, acoustic dispersion, and intersitium swelling are all potential candidates leading to improved distribution.

1.2.3 Controlling Ultrasound-Assisted Convection in Brain Tissue—Standing waves are well documented phenomena formed by the constructive interference of two mechanical waves traveling in opposite directions, including ultrasound waves propagating in a medium. The constructive interference of two equal and opposite waves, and the formation of a standing wave results in an interference pattern with nodes and anti-nodes that do not move in space temporally. The anti-nodes represent the peak positive and negative pressure of the ultrasound wave, whereas the nodes represent areas of no acoustic pressure from the ultrasound wave. Standing waves are commonly formed when an ultrasound source of consistent frequency and position, continuously generates an incident wave which then interferes with its own reflection off a boundary.

Standing waves have been exploited in a number of applications, biomedical and otherwise. Some examples include using ultrasonic standing waves to immobilize cells in a gel matrix at areas of minimal acoustic pressure (nodes) in the standing wave field as well as creating a physical force field filter within microfluidic devices [30, 31]. However, it is generally believed that standing waves in brain tissue are undesirable since localized high energy sites at the anti-nodes could cause damage to neuronal tissue. At the 1–2 MHz frequencies in particular, the wavelength is similar to the dimension of an artery in the brain, which could prove problematic if high energy spots were formed on this scale [32].

Research of *in vivo* brain drug delivery has utilized 1.34 MHz ultrasound in conjunction with CED to infuse Evans blue dye directly into the rat brain caudate. The results are generally a distribution volume of dye with a spherical or ellipsoid shape as shown in Figure 4. However, in anecdotal cases of UCED experimentation, distinct, non-continuous bands of dye are sometimes observed in brain sections close to the needle track and directly above the ultrasound transducer mounted on the brain as shown in Figure 5B. This phenomenon could be attributed to the formation of a standing ultrasound wave within the rat brain during the UCED infusion. This formation is likely the result of the incident ultrasound waves interfering with reflections from the rodent skull generating a steady spatial field of nodes and anti-nodes.

The observed banding is analogous to other processes whereby material accumulates in a standing wave field. However, the exact mechanism in brain tissue has not yet been identified. One possibility is that the tracer accumulates in the nodes, or the areas of least acoustic pressure. The other possibility is that the tracer accumulates at the anti-nodes where the ultrasound waves have the greatest amplitude. This increased energy could cause increased tissue permeability, causing tracer to preferentially accumulate at the anti-nodes.

To better understand whether tracer is accumulating at the nodes or anti-nodes, we calculated the wavelength of ultrasound in brain tissue and compared the result to the distance between the bands,

$$f=\frac{c}{\lambda} \tag{4}$$

where f is the frequency, c is the speed of sound in brain tissue (1460 m/s, [33]), and λ is the wavelength. We calculated the wavelength to be 1.09 mm, resulting in a node to node distance of 0.545 mm. The distance between the bands in the two experiments experiencing this phenomena are approximately 0.6 mm. It is likely that the accumulation of dye is at the node, similar to *ex vivo* standing wave experiments.

Though this result runs counter to the objective of maximizing volume distribution of an infusate as discussed in sections 1.2.1 and 1.2.2, it may have other applications. For instance, if various standing wave patterns or controlled acoustic fields were induced during an infusion, greater spatial and temporal control over the infusion could be achieved; this control could prove especially valuable with highly toxic targeted treatments. Difficulty arises in reproducing these *in vivo* results. Inducing a standing wave depends on correct alignment in the desired geometry as well as the correct ultrasound frequency. Inducing such a standing wave field *in vivo* would likely require real-time imaging and precise positioning of the ultrasound source. However, if standing waves prove harmful to the brain, measures can be taken to prevent their formation, such as randomizing frequency or moving the source [34].

Perhaps the most important implication of this observation of standing waves is that it lends supporting evidence showing that ultrasound is not only having an effect on brain tissue, but that ultrasound also directly affects the distribution profile of the infusate during CED. Advancing the knowledge of how ultrasound can affect the infusion profile will allow for the parameters governing UCED to be optimized as it evolves into a clinically relevant therapy for neurological disorders.

1.3 Time Reversal Acoustics (TRA)

Accurate focusing of ultrasonic waves is a fundamental aspect of most medical applications of ultrasound. The efficiency of ultrasound focusing in biological tissues is often limited by spatial heterogeneities in sound velocity in tissues and by the presence of reflective surfaces and boundaries. Refraction, reflection and scattering of ultrasound in inhomogeneous media can distort a focused ultrasound field. There are many methods of improving ultrasonic focusing in complex media based on phase and amplitude corrections in the focusing system, but they are often too complicated, and in some cases do not provide the necessary improvement.

An alternative, simple and elegant technique of focusing acoustic energy in inhomogeneous media is based on the concept of Time-Reversal Acoustics (TRA). This technique of focusing ultrasonic waves is based on the reversibility of acoustic propagation, which implies that the time-reversed version of an incident pressure field naturally refocuses on its source [35, 36]. Remarkably, numerous reflections from boundaries and internal structures, which may greatly limit and even completely diminish conventional focusing using a phased array, lead to the improvement of focusing in the TRA system [37, 38]

A diagrammatic example is shown in Figure 6 comparing the differences of TRA to phased-array focusing. Different applications of the TRA technique have been explored in varied domains [35, 39–41]

The inventor of the TRA focusing methods, Mathias Fink from the University of Paris, demonstrated the capability of TRA to provide spatial control and focusing of an ultrasonic beam in inhomogeneous media. One application of TRA explored by Fink et al. is related to ultrasonic hyperthermia through an intact skull. The challenge is to focus through the skull bone, which induces severe refractions and scattering of the ultrasonic beam. The TRA focusing technique allowed focusing and steering through the skull of an ultrasonic beam that converged in a 1.5 mm diameter spot with very low side lobes [42, 43].

TRA focusing relies on obtaining an initial signal from the target area. This requirement of having a beacon (e.g. a hydrophone) in the target region limits TRA applications. The “smart needle” solves this problem during a CED infusion: a transducer mounted in the tip of the needle that is used to infuse drugs into the brain provides the necessary feedback signal for establishing the TRA relationship between the transmitter and the site in the brain where the drug is infused.

In contrast to conventional ultrasound focusing techniques, TRA focusing allows concentration of acoustic energy not only in space but also in time. That is, the duration of the high intensity ultrasonic pulse in the focal point of the TRA device can be several orders of magnitude shorter than the transmitted signal. Such temporal compression of ultrasound signal makes it possible to use lower power ultrasonic systems than conventional systems for ultrasound therapy.

The purpose of this study was to develop, test and evaluate an ultrasonic device based on TRA principles for increasing the diffusion and convection of compounds in the brain during CED. The TRA focusing system uses a “smart needle” to provide highly accurate focusing of ultrasound in targeted tissue, thus minimizing ultrasound exposure of healthy tissue. Despite the fact that gliomas are the most common form of brain cancer, there have been few therapeutic advances in recent decades. Thus, if new technology such as the TRA ultrasound focusing system can be shown to improve the outcome of innovative therapies such as CED, it would have significant medical impact on thousands of patients.

2. METHODS

2.1 Technology Development

The schematic and TRA-UCED system developed for brain infusions is shown in Figure 7. The heart of the system is a microprocessor controlled custom designed TRA electronic unit with MatLab® interface and set of TRA reverberators/transmitters developed for the specific purpose. The electronic unit controls and monitors the power amplifier, reverberator and ultrasound focusing beacon “smart needle”. Depending on exposure and application, the number of transmitting channels in the TRA-UCED system may be varied from 1 to 10. Increasing the number of transmitting channels from the reverberator improves the focusing ability of the TRA-UCED system and provides flexibility in controlling the acoustic energy at focal area.

The waveform generator of the TRA electronic unit generates the initial excitation signal with a predefined waveform and applies it to each channel of the reverberator one after another. The TRA electronics records the signals measured from the smart needle, which is located where the ultrasound needs to be focused (i.e. the brain). The recorded set of signals is then time-reversed, amplified, synchronized and applied simultaneously to all transducers of the transmitter. The resulting acoustical signals accurately focus at the target point. One of the advantages of the TRA-UCED focusing system is the opportunity to focus signals of different forms and spectra [44]. The ability to flexibly control the temporal and spectral

content of focused ultrasound could be important for ultrasound-assisted convection enhanced delivery.

2.1.1 Hydrophone Infusion Catheter "Smart Needle"—The smart needle was designed to work with the TRA electronics as well as typical CED infusion equipment. The needle-hydrophone was positioned on a stereotaxic control arm with standard BNC connector to act as the TRA-UCED smart needle. The challenge with the design was scaling down the needle-hydrophone to be small enough in diameter to allow for successful infusion into the rodent brain as well as maintain adequate sensitivity and robustness for multiple uses.

The final design solution to this problem was a novel longitudinal resonating piezo with center frequency of 1 MHz positioned internal to the needle. The piezo transducer was connected with micro coax cable through the side wall of the 30 gauge stainless steel blunted cannula, which was mounted onto a guide-assembly. Electrical connections were made through the aluminum guide-assembly, while fluid connections were made with micro peek tubing at the top of the needle as show in in Figure 8A. The smart needle for the TRA-UCED system was calibrated with a hydrophone from Onda Inc. providing a sensitivity of 2.63×10^{-6} V/Pa at 1 MHz.

2.1.2 TRA-UCED Reverberator—The therapeutic TRA-UCED reverberator was constructed to provide accurate focusing of 1 MHz center frequency excitation and deliver a broad therapeutic acoustic intensity range. It was made of aluminum, due to its low sound attenuation factor. Even though the skull itself constitutes an excellent reverberant cavity that might render the use of an external reverberator unnecessary, we decided to use an external reverberator because of the small size of the rodent head which limited the number of piezo discs that could be attached directly to the skull, and the relatively small surface area for acoustic coupling. Furthermore, the advantage of an external reverberator was that it allowed us to use multiple transducers in a randomized pattern, which was important in providing sufficient acoustic energy and focusing. A number of reverberators were manufactured and tested to optimize the design suited for the animal studies. Both solid and liquid filled designs with piezo discs of different frequencies were considered [45]. The length of reverberator and number of piezo discs were also optimized to provide the best focusing and pressure amplitude in the rat skull.

The reverberator developed and employed in this study is shown in Figure 9. It was designed with low impedance principles to work efficiently with the power amplifier discussed in *section 2.1.3* and was constructed to meet the experimental limitations in the size of the rodent head and surgical stereotaxic frame. The ultrasound therapy reverberator was designed with parallel configurations of 18 piezoelectric crystals with two 1 MHz PZT-4 piezoelectric crystals composing each individual TRA focusing channel. The reverberator was supported by a plastic control arm with ball and socket wobbler arranged on an aluminum shaft for control and maneuverability. The shaft was mounted to a magnetic foundation to secure the transducer in various configurations for delivery of TRA-UCED to the rodent brain.

2.1.3 Ten Channel Ultralow-Impedance Power Amplifier—The principles underlying the technology and construction of battery powered efficient ultrasound systems have been described elsewhere [46–50]. Here, we developed a new ultralow output ultrasound impedance ultrasound driver design, based on a 16 Power MOSFET per channel, surface mount component and printed circuit board (PCB) design for application in TRA-UCED to the brain. Each channel was designed to work with TRA computer and focusing electronics and hardware, and able to provide continuous wave (CW), frequency sweep and

variable duty cycle capability for driving the ultrasound reverberator for DC-3 MHz TRA-UCED applications.

The amplifier is shown at various stages of development in Figure 10. The ultralow output impedance 10 channel ultrasound amplifier was constructed using two six layer printed circuit boards (PCB) 1 × 18 inches in size created with PCB123® Layout V2 software from Sunstone Circuits Inc. Mulino, OR. The circuit architecture of 16 complimentary N/P parallel MOSFETs in transistor-transistor logic (TTL) timing configuration for each independent channel provides efficient voltage transfer from the driver to the TRA-UCED reverberator. Each PCB has a total of 5 independent channels that were populated in-house due to the simplicity of the design. The parts list for each PCB included approximately 80 MOSFETs, 30 PIN drivers, 200+ capacitors and resistors, 40 heat sinks, 10 fans, 5 BNC connectors, 5 voltage regulators, 5 LEDs and other miscellaneous components. Figure 10 A and B show the PCB 5-channel modules, two of which make up each 10-channel power amplifier shown in C.

The amplifier is powered by two +/− 30 V 10 Amp power supplies that control the power to the reverberator, and one 8 V 2 Amp power supply that enables the fans, integrated circuits and general amplifier functionality. The BNC input of the amplifier accepts 2 to 5 volt transistor-transistor logic signals supplied by the TRA electronic unit and amplifies the signal up to a maximum of +/− 30 volt push-pull square wave drive signal. The output of the each amplifier channel is connected to ultra-flexible coax cable terminated with a female BNC connector. Each channel can supply over 50 watts of electrical energy to power the reverberator over a large acoustic therapeutic range.

2.1.4 Electronic Unit, Data Acquisition and Processing Algorithms and Software—The core of the TRA-UCED system is the microprocessor controlled, custom designed TRA electronic unit developed for various medical and industrial applications. For the TRA-UCED system a parallel architecture 10 channel TRA electronic unit was constructed for superior control options, faster operation and data transfer, compact design and low power consumption. The TRA electronics generates the initial TTL excitation signal applied to each channel of the power amplifier and then to each channel of the TRA reverberator, records the signal measured by a needle-hydrophone smart needle placed at the desired location for focusing i.e. the brain, amplifies and inverts the signal in time, and applies this time reversed signal back to the amplifier to send focused ultrasound to the beacon. An internal clock of the electronic unit provides multiple sampling frequency capability in range 2.5 MHz to 40 MHz. It communicates with the PC through a 2 channel USB2 interface, and is capable of operation with up to 95% duty cycle.

User control of the TRA-UCED system is based on a MatLab® USB interface to the TRA electronics. The low-level software for data acquisition and processing was designed as a set of functions internal to the high-level software developed for flexibly controlling the ultrasound exposure parameters in the treatment area. The graphical user interface (GUI) for the TRA-UCED system is shown in Figure 11. The high-level program is initiated in the MatLab® command window using the function call to the main program TRA_UI(`expert'). This function initializes the entire TRA-UCED system and collects the required time-reversed signal from reverberator to smart needle for focusing ultrasound. Once initialized, the GUI enables the selection of frequency, pulse duration, pulse repetition, duty factor for the duration of the experiment in real time. The program can also automatically find the optimum parameters such as frequency, number of pulses and pulse duration. The program implements an automatic recalibration routine to collect the time-reversed signal for re-focusing if the acoustic pressure or intensity drops below the user defined threshold.

The GUI provides complete control of the ultrasound energy at the focal area to activate microbubble stable cavitation and enhance interstitial drug transport without causing tissue damage. A wide range of ultrasound exposure parameters like frequency, pulse duration and repetition, duty factor, and different commercially available microbubbles were explored to begin optimization of the desired effect. Further information on the TRA electronic system and results on studies can be found in [23, 39, 40–45, 51–56].

3. RESULTS

3.1 In Vitro Evaluation

The TRA-UCED system was evaluated in the fluid-filled rodent skull with a smart needle attached to the 3D positioning system (Figure 12A). Figure 12B shows the spatial distribution of the intensity of the 1-MHz focused ultrasound by the smart needle. The TRA-UCED system provided 1.5 mm spatial focusing resolution in the rodent skull with a signal to noise ratio (SNR) of approximately 5. The studies also confirmed the capability of the developed reverberator to provide intensity levels required inside the rat brain for enhanced convection discussed in 1.2.1

3.2 In Vivo Evaluation

3.2.1 Animal, Ultrasound and Infusion Protocol—Rats were anesthetized and euthanized by procedures approved by the Institutional Animal Care and Use Committee (IACUC) at Cornell University. A total of 50 Sprague–Dawley rats (350 to 450 g) were divided into five power ranging groups to study Convection Enhanced Delivery (CED) infusion distribution with Ultrasound (UCED). Animals were anesthetized by inhalation of isoflurane gas, the head was shaved and secured in a stereotaxic frame. 0.1 ml of bupivicaine was applied under the skin as a local anesthetic and an incision was made in the skin along the dorsal midline of the skull. A small craniotomy (2–4 mm diameter) was made over the left side of the exposed skull using a dental drill. The ultrasound therapy transducer resonator was positioned on the right intact skull of the rodent with acoustic coupling made using ultrasound gel and secured into position. The smart needle was then guided using a micromanipulator to +0 mm anterior, +3 mm lateral and −5.5 mm ventral from bregma, lowered at 0.25 mm per second into the caudate of the rat brain and allowed to equilibrate for two minutes. The TRA-UCED system was powered up with various amplifier +/− voltage settings and Matlab® computer interface initialized. Once the TRA-UCED program was running, the pulse sequence and repetition rate parameters of the ultrasound therapy were standardized to 16 μs bursts repeated 20 times with 250 ms intervals. Delivery of ultrasound energy was then engaged and infusion began (Figure 13).

For each rat, the entire experiment lasted a total of 30 min. The control groups of CED and CED+MicroBubbles (MB) (n=5 in each) were infused using the smart needle with no ultrasound therapy for 30 min. For the experimental groups of TRA-UCED and TRA-UCED + MB (n=2 to 5 in each), infusion and ultrasound exposure at amplifier voltage settings of +/− 2, 6, 10, 20 and 25 volts, corresponding to acoustic intensities ranging from 0.307 to 30.1 mW/cm^2, was applied simultaneously. Filtered Evan's blue dye (EBD) 0.25 wt% in phosphate buffered saline (PBS) without or with 5×10^5 stabilized microbubbles per μL with median diameter of 2.5 μm (Targestar P, Targeson Inc. San Diego, CA) was infused using a microinfusion pump (Worker Bee, BASi Inc. West Lafayette, IN). The starting infusion flow rate for the experiments was 0.1 μL/min for 5 min, the infusion flow rate was then increased to 0.2 μL/min for an additional 5 min, to the final flow rate of 0.5 μL/min for 20 min. After 30 min of simultaneous infusion and ultrasound therapy the experiment was stopped. The smart needle and ultrasound therapy transducer reverberator were left in place for 1–2 min before being removed while euthanasia via cardiac urethane injection was

performed. The animal was then removed from the stereotaxic frame and immediately perfused with 200 mL of PBS followed by 200 mL 4% paraformaldehyde fix. The brain was then promptly removed from the skull using bone cutters and prepared for frozen section in 30% sucrose and 4% paraformaldehyde solution for one day, and moved to 60% sucrose and 4% paraformaldehyde solution for another day, before being frozen on dry ice in Optimal Cutting Temperature (OCT) compound (Sakura Tissue Tek Inc. Torrance, CA) in preparation for frozen section.

3.2.2 Data Collection—Tissue slices were imaged using a CCD camera (Canon Power Shot G10, Canon Inc. Lake Success, NY) arranged on a cryostat (Microm HM 550, ThermoFisher Scientific Inc. Waltham, MA) during frozen section through the brain in the coronal plane. The high resolution 14 Mpix Joint Photographic Experts Group (JPEG) image files were captured at the first visualization of EBD in the brain tissue and in 250 μm intervals thereafter until EBD was no longer distinguishable. The digital image files were cropped to include the rodent brain with a white ring of OCT compound around its outside and resized to 300 × 210 pixels with a locked aspect ratio using Adobe® Photoshop®.

An excerpt from the data collected is shown in Figure 14 with a typical CED infusion of EBD only in the center, and TRA-UCED and TRA-UCED + MB on the left and right side of the figure, respectively. With an increase in amplifier voltage and increase in acoustic energy being delivered to the smart needle, a corresponding increase of EBD volume distribution and reduction of reflux along the smart needle tract is found for TRA-UCED and TRA-UCED + MB groups studied. For the parameters examined, TRA-UCED groups at the highest voltage setting of +/− 25 V and acoustic intensity of 30.1 mW/cm^2 provided the greatest increase of volume distribution as compared to other experimental groups. The addition of micro bubbles to the infusate during ultrasound exposure resulted in visual increases in EBD distribution at lower acoustic intensities as compared to non-microbubble groups.

Preliminary analysis of the TRA-UCED power range data sets show that only short bursts of ultrasound may improve distribution volumes, however quantification of these data sets is required. Furthermore, current exposure levels for TRA-UCED have shown no histological difference between ultrasound groups and controls in acute experiments.

4. CONCLUSIONS

In this study we successfully developed and preliminarily tested a 10 channel time-reversal based focusing system to deliver therapeutic ultrasound to the tip of a cannula during convection enhanced drug delivery to the brain. The TRA-UCED system was able to accurately focus 1 MHz ultrasound in the rodent skull *in vitro* as well as focus during CED infusion of Evans blue dye into the rodent caudate *in vivo*. The TRA-based focusing approach provided accurate ultrasound delivery to the cannula tip with 1.5 mm resolution (Figure 12) using a focusing system no larger than a small desktop computer (Figure 7).

The system and results presented show that time-reversal acoustic principles have potential to be applied to biomedical situations of ultrasound focusing without the need for complex transducer phased arrays and the electronics to control multiple channels. Furthermore, delivering only small bursts of ultrasound energy every second over the 30 min experiment to the needle tip, while simultaneously infusing tracer into the brain parenchyma through the needle showed ultrasound enhanced volume distribution over control infusions (Figure 14).

From the results presented, we find that 1 MHz time-reversal focused ultrasound is a promising new method to increase the penetration of small molecular weight drugs into

brain tissue. The eventual goal of this work will be to use ultrasound to drive locally delivered chemotherapy agents past current diffusion and convection limitations to target and reach migratory cancer cells. Continued research to study how changes in ultrasound parameters will affect the rate and level of tracer penetration in animal brain tissues will be important to optimize exposure levels. Reverberators of different frequencies and TRA-UCED delivery at different acoustic intensities and pulse sequences appropriately below the brain tissue damage threshold should be explored to create a therapeutically useful regime. Furthermore, the ability of TRA focusing to develop unique focal volumes of arbitrary shape for directing and targeting therapeutics in the brain parenchyma should be explored.

Acknowledgments

The authors thank Dr. Nozomi Nishimura and Prof. Chris Schaffer of the Department of Biomedical Engineering, Cornell University for use of the Schaffer Labs animal surgery suite.

This research was supported by The New York Brain Tumor Project of Weill Cornell Medical College and National Institutes of Health Grant #1R43NS065524-01.

REFERENCES

1. Bobo RH, Laske DW, Akbasak A, Morrison PF, Dedrick RL, Oldfield EH. Convection-enhanced delivery of macromolecules in the brain. Proc. Natl. Acad. Sci. USA. 1994; 91(6):2076–2080. [PubMed: 8134351]
2. Vogelbaum MA. Convection enhanced delivery for treating brain tumors and selected neurological disorders: symposium review. J. Neurooncol. 2007; 83(1):97–109. [PubMed: 17203397]
3. Lonser RR, Gogate N, Morrison PF, Wood JD, Oldfield EH. Direct convective delivery of macromolecules to the spinal cord. J. Neurosurg. 2001; 89(4):616–622. [PubMed: 9761056]
4. Wood JD, Russell BS, Lonser R, Gogate N, Morrison PG, Oldfield EH. Convective delivery of macromolecules into the naïve and traumatized spinal cords of rats. J. Neurosurg. 1999; 90(Suppl 1):115–120. [PubMed: 10413135]
5. Lonser RR, Corthésy MW, Morrison PF, Gogate N, Oldfield EH. Convection-enhanced selective excitotoxic ablation of the neurons of the globus pallidus internus for treatment of parkinsonism in nonhuman primates. J. Neurosurg. 1999; 91(2):294–302. [PubMed: 10433318]
6. Fiandaca MS, Forsayeth JR, Dickinson PJ, Bankiewicz KS. Image-guided convectionenahnced delivery platform in the treatment of neurological diseases. Neurotherapeutics. 2008; 5(1):123–127. [PubMed: 18164491]
7. Lonser RR, Schiffman R, Robison RA, Butman JA, Quezado Z, Walkter ML, Morrison PF, Walbridge S, Murray GJ, Park DM, Brady RO, Oldfield EH. Image-guided, direct convective delivery of glucocerebrosidase for neuronopathic Gaucher disease. Neurology. 2007; 68(4):254–261. [PubMed: 17065591]
8. Rainov NG, Soling A, Heidecke V. Novel therapies for malignant gliomas: a local affair? Neurosurg. Focus. 2006; 20(4):E9. [PubMed: 16709040]
9. Neeves KB, Sawyer AJ, Foley CP, Saltzman WM, Olbricht WL. Dilation and degradation of the brain extracellular matrix enhances penetration of infused polymer nanoparticles. Brain Res. 2007; 1180:121–132. [PubMed: 17920047]
10. Sarntinoranont M, Chen X, Zhao J, Mareci TH. Computational model of interstitial transport in the spinal cord using diffusion tensor imaging. Ann. Biomed. Eng. 2006; 34(8):1304–1321. [PubMed: 16832605]
11. Mitragotri S, Blankschtein D, Langer R. Ultrasound-mediated transdermal protein delivery. Science. 1995; 269(5225):850–853. [PubMed: 7638603]
12. Boucaud A, Garrigue MA, Machet L, Vallant L, Patat F. Effect of sonication parameters on transdermal delivery of insulin to hairless rats. J. Cont. Release. 2002; 81(1–2):113–119.
13. Machet L, Boucaud A. Phonophoresis: efficiency, mechanisms and skin tolerance. Int. J. Pharm. 2002; 243(1–2):1–15. [PubMed: 12176291]

14. Mitragotri S, Kost J. Low-frequency sonophoresis: a review. Adv. Drug Deliv. Rev. 2004; 56(5): 589–601. [PubMed: 15019748]
15. ter Haar G. Therapeutic applications of ultrasound. Prog Biophys Mol Biol. 2007; 93(1–3):111–129. [PubMed: 16930682]
16. Guzman HR, Nguyen DX, McNamara AJ, Prausnitz MR. Equilibrium loading of cells with macromolecules by ultrasound: Effects of molecular size and acoustic energy. J. Pharm. Sci. 2002; 91(7):1693–1701. [PubMed: 12115831]
17. Keyhani K, Guzman HR, Parsons A, Lewis TN, Prausnitz MR. Intracellular drug delivery using low-frequency ultrasound: Quantification of molecular uptake and cell viability. Pharm. Res. 2001; 18(11):1514–1520. [PubMed: 11758757]
18. Hynynen K, Clement G. Clinical applications of focused ultrasound - The brain. Int. J. Hyperth. 2007; 23(2):193–202.
19. Patrick JT, Nolting MN, Goss SA, Dines KA, Clendenon JL, Rea MA, Heimburger RF. Ultrasound and the blood brain barrier. Adv. Exp. Med. Biol. 1990; 267:369–381. [PubMed: 2088054]
20. Lewis GK Jr. Olbricht WL. A phantom feasibility study of acoustic enhanced drug perfusion in neurological tissue. Proc. IEEE, LISA. 2007:67–70.
21. Lewis GK Jr. Olbricht WL, Lewis GK Sr. Acoustic targeted chemotherapy in neurological tissue. J. Acoust. Soc. Am. 2007; 122:3007. abstract.
22. Lewis GK Jr. Wang P, Lewis GK Sr. Olbricht WL. Therapeutic ultrasound enhancement of drug delivery to soft tissues. 8th Int. Sym. Ther. Ultras. AIP conf. Proc. 2008; 1113:403–407.
23. Lewis GK Jr. Filinger L, Lewis GK Sr. Olbricht WL, Sarvazyan A. Time-reversal techniques in ultrasound-assisted convection-enhanced drug delivery to the brain: Technology development and in vivo evaluation. J. Acoust. Soc. Am. 2010; 128:2335.
24. Liu Y, Paliwal S, Bankiewicz KS, Bringas JR, Heart G, Mitragotri S, Prausnitz MR. Ultrasound-enhanced drug transport and distribution in the brain. AAPS PharmSciTech. 2010; 11(3):1005–1017. [PubMed: 20532711]
25. Lewis, GK, Jr.. Medical Ultrasound for Brain Drug Delivery and Rehabilitation Medicine. Ph.D. Thesis. Cornell University; 2011.
26. Fung LK, Shin M, Tyler B, Brem H, Saltzman WM. Chemotherapeutic drugs released from polymers: Distribution of 1,3-bis(2-chloroethyl)-1-nitrosourea in the rat brain. Pharma. Res. 1996; 13(5):671–682.
27. Fung LK, Ewend MG, Sills A, Sipos E, Thompson R, Watts M, Colvin OM, Brem H, Saltzman WM. Pharmacokinetics of interstitial delivery of carmustine, 4 hydroperoxycyclophosphamide, and paclitaxel from a biodegradable polymer implant in the monkey brain. Cancer Res. 1998; 58(4):672–684. [PubMed: 9485020]
28. Saltzman, WM. Drug delivery: Engineering principles for drug therapy. Oxford University Press; Oxford: 2001.
29. Brightman MW. The brain's interstitial clefts and their glial walls. J. Neurocytol. 2002; 31(8–9): 595–603. [PubMed: 14501201]
30. Gherardini L, Cousins CM, Hawkes JJ, Spengler J, Radel S, Lawler H, Devcic-Kuhar B, Groschl M, Coakley WT, McLoughlin AJ. A new immobilization method to arrange particles in a gel matrix by ultrasound standing waves. Ultrasound in Med. & Biol. 2005; 31(2):261–272. [PubMed: 15708466]
31. Hawkes JJ, Coakley WT. Force field particle filter, combining ultrasound standing waves and laminar flow. Sensors and Actuators B: Chemical. 2001; 75(3):213–222.
32. Culp WC, McCowan TC. Ultrasound augmented thrombolysis. Current Medical Imaging Reviews. 2005; 1:5–12.
33. Goss SA, Johnston RL, Dunn F. Compilation of empirical ultrasonic properties of mammalian tissues. J. Acoust. Soc. Am. 1980; 68:93–108. [PubMed: 11683186]
34. Tang SC, Clement GT. Standing wave suppression for transcranial ultrasound by random modulation. IEEE Trans Biomed Eng. 2010; 57(1):203–205. [PubMed: 19695991]
35. Fink M, Montaldo G, Tanter M. Time reversal acoustics in biomedical engineering. Ann. Rev. Biomed. Eng. 2003; 5:465–497. [PubMed: 14527319]

36. Sutin, A.; Sarvazyan, A. Spatial and temporal concentrating of ultrasound energy in complex systems by single transmitter using time reversal principles. Proc. World Congress on Ultrasonics; Paris, France. 2003. p. 863-866.
37. Tanter M, Thomas JL, Fink M. Focusing and steering through absorbing and aberrating layers: application to ultrasonic propagation through the skull. J. Acoust. Soc. Am. 1998; 103:2403–2410. [PubMed: 9604342]
38. Thomas JL, Fink M. Ultrasonic beam focusing through tissue inhomogeneities with a time reversal mirror: Application to transkull therapy. IEEE Trans. Ultrason. Ferroelec. Freq. Contr. 1996; 43(6):1122–1129.
39. Sarvazyan AP, Fillinger L, Gavrilov LR. A comparative study of systems used for dynamic focusing of ultrasound. Acoustical Physics. 2009; 55(4–5):630–637.
40. Sarvazyan A, Fillinger L, Gavrilov L. Time-reversal acoustic focusing system as a virtual random phased array. IEEE Trans Ultrason Ferroelectr Freq Control. 2010; 57(4):812–817. [PubMed: 20378444]
41. Sutin A, Sarvazyan A. Advantages of time reversal acoustic focusing system in biomedical applications. J. Acoust. Soc. Am. 2005; 118:1941.
42. Sinelnikov, Y.; Sutin, A.; Zou, Y.; Sarvazyan, A. Time reversal acoustic focusing with liquid resonator for medical applications. Trans. 6th Intl. Symp. Ther. Ultrasound, Intl. Soc. Ther. Ultrasound; Oxford, UK. 2006, Aug. 30-Sept. 2; p. 82-86.
43. Sutin A, Libbey B, Fillinger L, Sarvazyan A. Wideband nonlinear time reversal seismo-acoustic method for landmine detection. J. Acoust. Soc. Am. 2009; 125(4):1906–1910. [PubMed: 19354365]
44. Choi BK, Sutin A, Sarvazyan A. Formation of Desired Waveform and Focus Structure by Time Reversal Acoustic Focusing System. Proc. of 2006 IEEE Ultrasonics Symp. 2006:2177–2181.
45. Sarvazyan A, Fillinger L. Arbitrary shaped, liquid filled reverberators with non-resonant transducers for broadband focusing of ultrasound using Time Reversed Acoustics. Ultrasonics. 2009; 49(3):301–305. [PubMed: 19062060]
46. Lewis GK Jr. Olbricht WL. Development of a portable therapeutic and high intensity ultrasound system of military, medical and research use. Rev. Sci. Inst. 2008; 79(11):1–9.
47. Lewis GK Jr. Olbricht WL. Development of a portable therapeutic ultrasound system for military, medical and research use. J. Acoust. Soc. Am. POMA. 2008; 5
48. Lewis, GK., Jr.; Olbricht, WL. Wave Generating Apparatus. UPCT Patent Application No. PCT/US2009/50297. 2009.
49. Lewis GK Jr. Olbricht WL. Design and characterization of a high-power ultrasound driver with ultralow-output impedance. Rev. Sci. Inst. 2010; 80(11):1–8.
50. Henderson P, Lewis GK Jr. Olbricht WL, Spector J. A portable high intensity focused ultrasound device for the non invasive treatment of varicose veins. J. Vas. Surg. 2010; 51(3):707–711.
51. Sutin A, Libbey B, Kurtenok V, Fenneman D, Sarvazyan A. Nonlinear detection of land mines using wide band width time-reversal techniques. Proc. SPIE. 2009; 6217:B1–B12.
52. Sinelnikov YD, Sutin AM, Vedernikov AY, Sarvazyan AP. Time reversal acoustic focusing with a catheter balloon. Ultrasound Med. Biol. 2010; 36(1):86–94. [PubMed: 19900754]
53. Sinel'nikov ED, Sutin AM, Sarvazyan AP. Time reversal in ultrasound focusing transmitters and receivers. Acoustical Physics. 2010; 56(2):183–193.
54. Fillinger L, Kurtenoks V, Lewis GK Jr. Sutin A, Sarvazyan A. Time reversal ultrasound system for enhanced drug delivery in rat brain. Proc. Int. Symp. Ther. Ultras. 2010; 1114:403–407.
55. Sarvazyan, A.; Fillinger, L.; Sutin, A. Focusing of broadband acoustic signals using time-reversed acoustics. USA Pat # 7,587,291. Issued 9/8/2009
56. Sarvazyan, A.; Emelianov, S. Wireless beacon for time-reversal acoustics, method of use and instrument containing thereof. USA Pat #7,713,200. Issued 05/11/2010

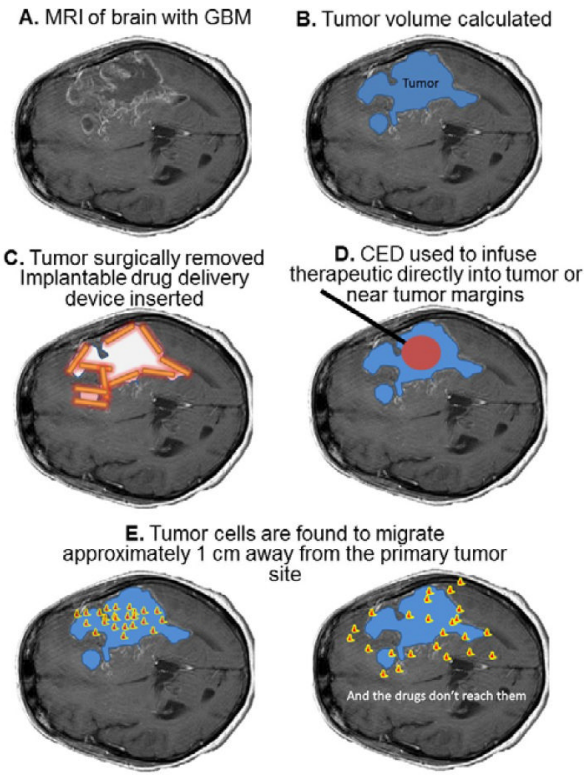

Figure 1.

Diagrammatic representation of glioblastoma multiforme. A. Magnetic Resonance Image (MRI) of brain, B. Tumor volume is calculated (in blue) and in some cases tumor is removed, C. The resection cavity may be lined with gliadel® wafers (in orange) with encapsulated chemotherapeutic, D. Convection Enhanced Delivery (CED) may be used to infuse chemotherapeutic (in red) through a cannula (in black) into the tumor, resection cavity, and/or around the resection cavity. E. In most cases another tumor will appear approximately 1 to 3 cm away from the original tumor site due to cell migration (depicted in red/yellow).

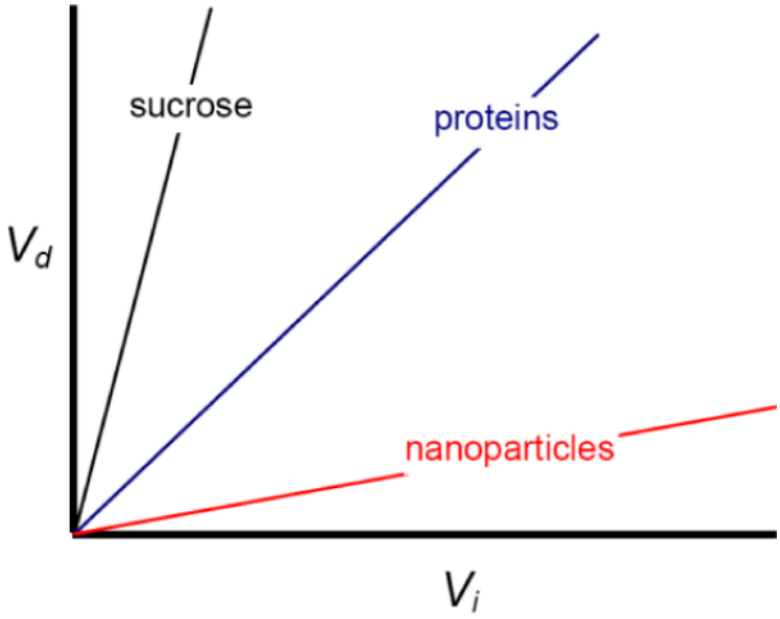

Figure 2.
Distribution volume as a function of infusion volume.

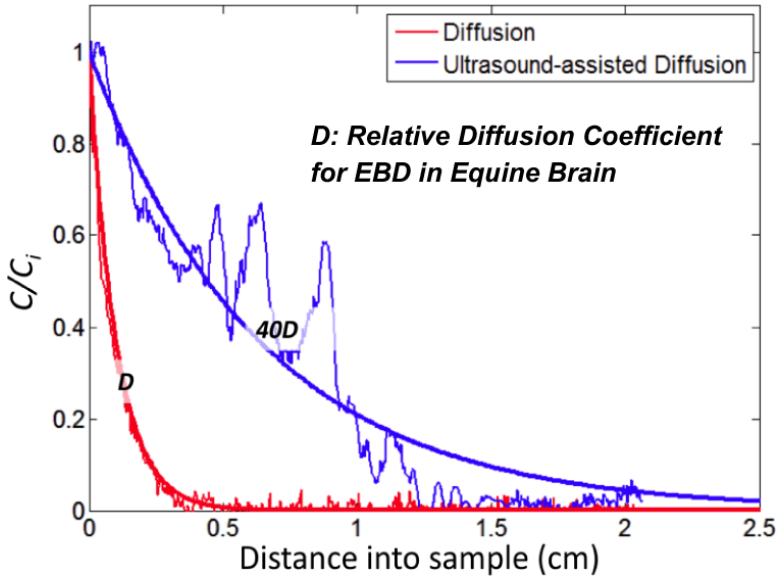

Figure 3.

EBD concentration profiles after 2 min in equine brain tissue without ultrasound (red) and with 1W/cm^2 ultrasound (blue) for 2 min. Ultrasound increases the apparent diffusion coefficient by about 40x.

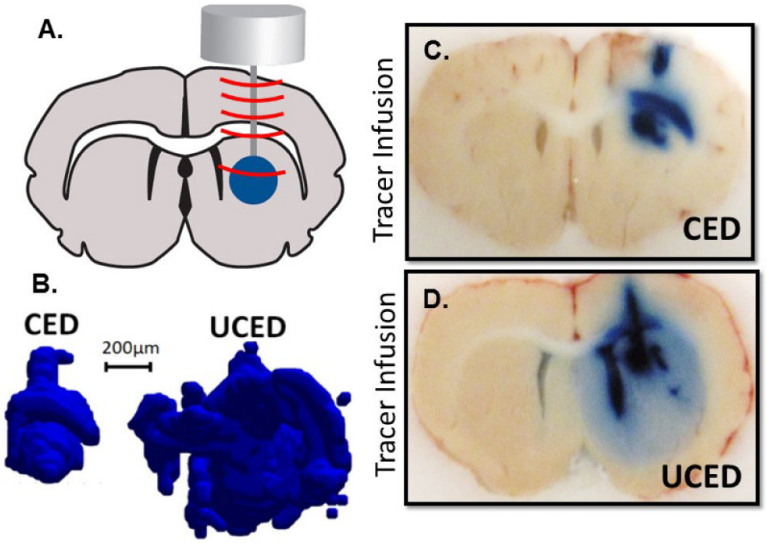

Figure 4.

Ultrasound-assisted Convection Enhanced Delivery (UCED) to the rodent brain. A. A plane wave transducer with cannula through-hole is mounted on top of the rodent brain through a small craniotomy window in the skull. Infusion at 0.5 uL/min of EBD with and without continuous wave ultrasound operating at $I=47mW/cm^2$ for 30 minutes. B. 3-dimensional reconstruction of infusion volume with (UCED) and without (CED) ultrasound exposure. C and D. Brain slices in the cannula path showing EBD distribution with (UCED) and without (CED) ultrasound exposure.

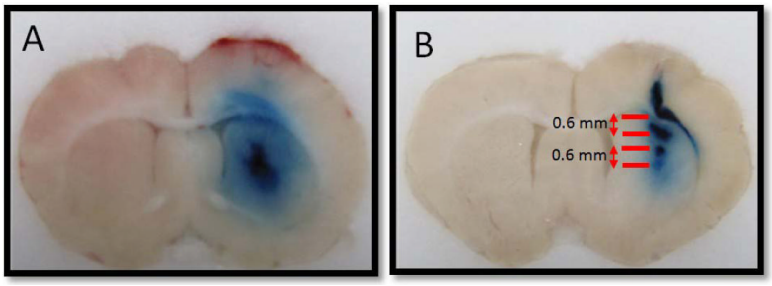

Figure 5.
Ultrasound-assisted Convection Enhanced Delivery (UCED) infusion profiles. The rat brain in (A) shows a relatively uniform distribution, while the brain in (B) shows clear banding of the infused dye approximately 0.6 mm apart.

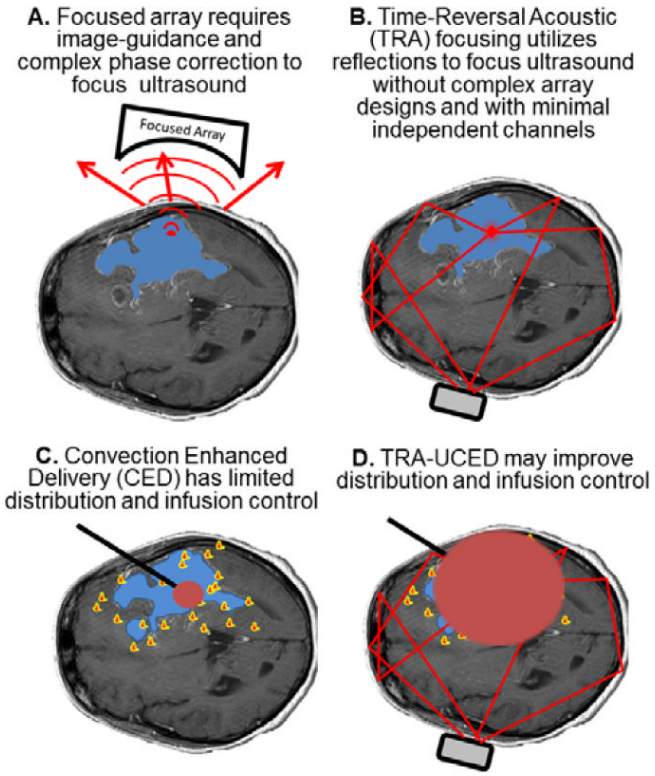

Figure 6.

Time-Reversal Acoustic (TRA) application for drug delivery in the brain. A. Focused arrays require complex phase correction and image-guidance to account for aberrations of the acoustic field by the skull. B. A simple reverberator placed on the outside of the skull and TRA principles may be used to focus energy with as little as one or two channels. C. Currently one of the largest limitations of CED is the ability to control the infusion (red) to target the migrating cancer cells (yellow/red). TRA-UCED may provide a minimally invasive approach to improve CED with transcranial delivery of ultrasound.

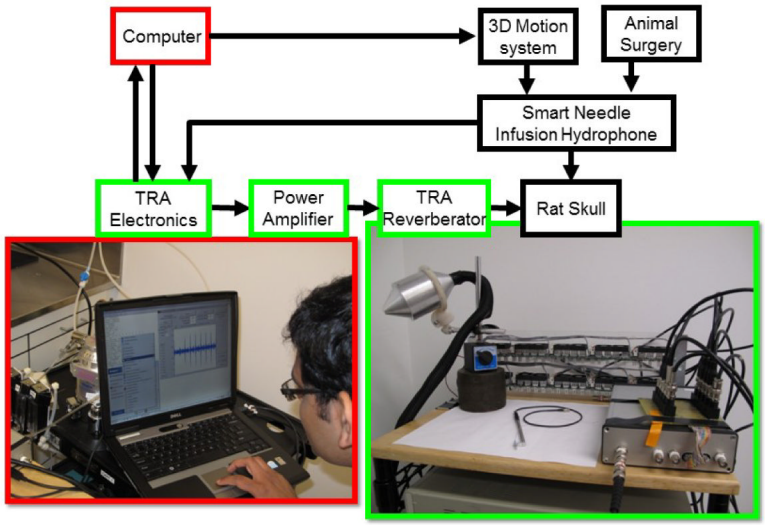

Figure 7.
Time-Reversal Acoustics Ultrasound-assisted Convection Enhanced Delivery (TRA-UCED) system.

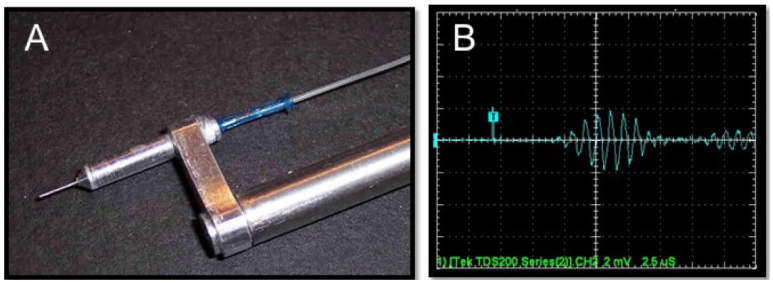

Figure 8.

Hydrophone infusion catheter “smart needle”: for TRA-UCED. A. The ultrasound element is internal to the lumen of the 30 gauge stainless steel cannula. Electrical connections are made through the stereotaxic guide arm while the infusate is connected with flexible tubing. B. The response of the hydrophone to 1 MHz signal is shown with sensitivity of 2.63×10^{-6} V/Pa

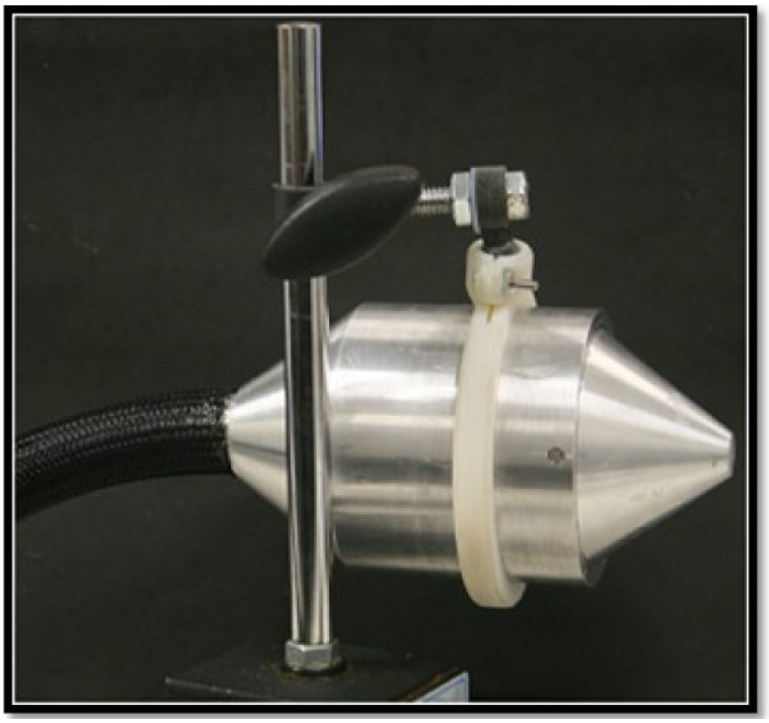

Figure 9.
Reverberator for delivering therapeutic ultrasound to the smart needle for TRA-UCED. Housed inside the aluminum cone are 18 piezoelectric 1 MHz disks oriented at random locations and angles that make up the nine independent channels. The nose cone tapers down for easy placement onto the rodent head during TRA-UCED.

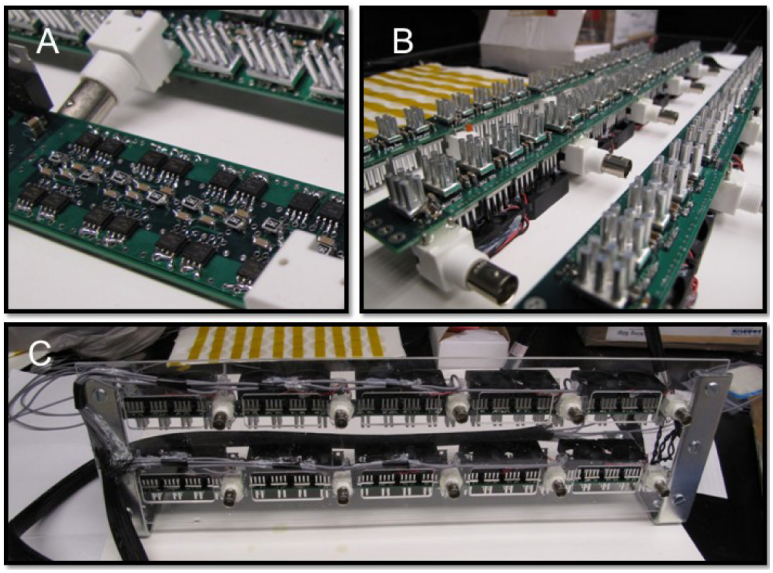

Figure 10.
Ultralow-impedance 10 channel +/− 30 V push-pull amplifier. A. Close up of one channel with 16 power MOSFETs arranged on the outside of the PCB. B. Fully populated PCBs with thermal management heat sinks and fans. C. Finished 10 channel power amplifier with BNC inputs on the front panel, and coax-cable outputs on left side.

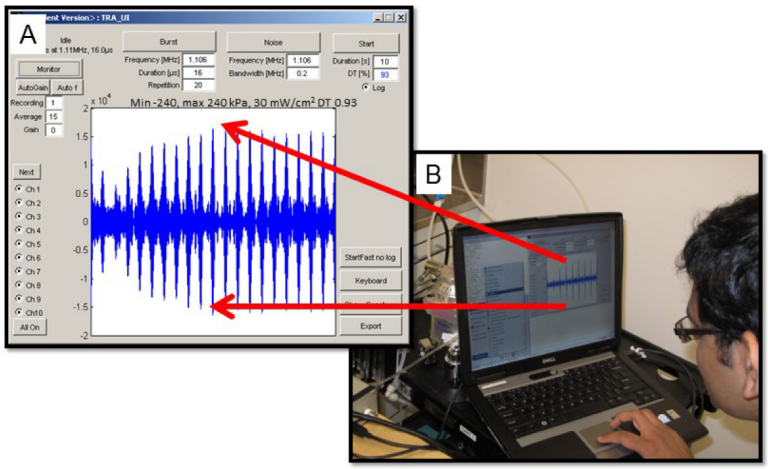

Figure 11.
TRA-UCED MatLab® interface and user control center. A. Screen shot of graphical user interface and focusing of multiple +/− 240 kPa 1.1 MHz ultrasonic pressure waves to the smart needle. B. PC-based computer running the TRA-UCED system in the laboratory.

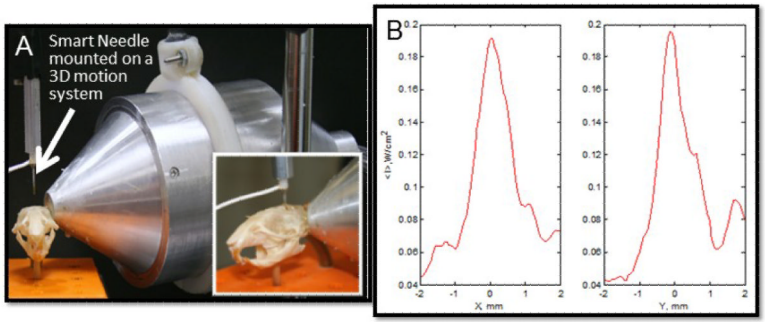

Figure 12.

A. The TRA-UCED system positioned on the rodent skull for preliminary focusing measurements B. Results show that the system provides 1.5 mm focusing resolution in the rodent skull on both the x and y axis of the sagittal plane.

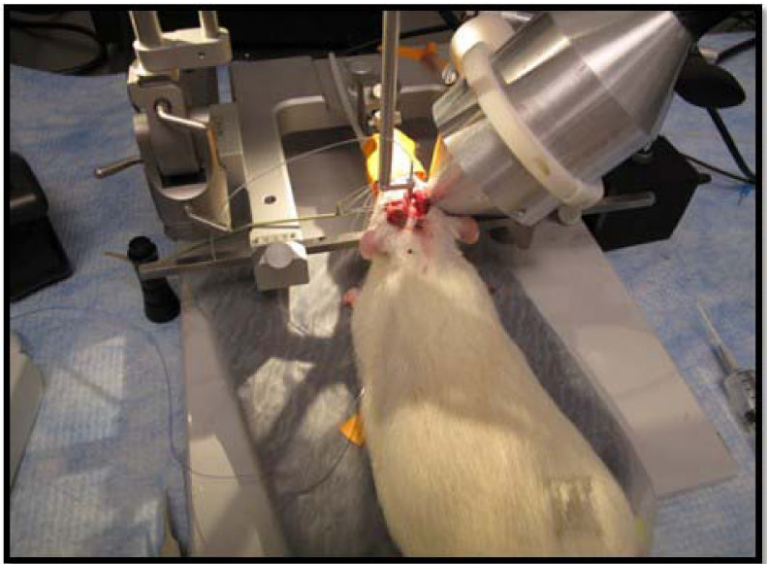

Figure 13.
TRA-UCED experimental *in vivo* setup. Rodent is secured on stereotaxic device, reverberator coupled to rodent skull and smart needle inserted into rodent caudate.

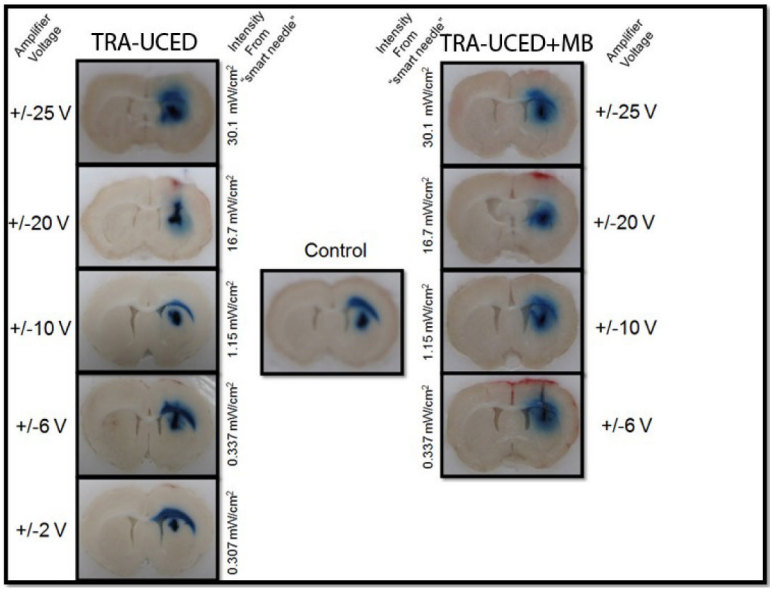

Figure 14.
Time-Reversal Acoustic Ultrasound-assisted Convection Enhanced Delivery (TRAUCED). Increasing the acoustic intensity shows increases in tracer distribution volume.